

<https://helda.helsinki.fi>

Retinal Pigment Epithelial Cell Line with Fast Differentiation and Improved Barrier Properties

Hellinen, Laura

2019-08

Hellinen , L , Pirskanen , L , Tengvall-Unadike , U , Urtti , A & Reinisalo , M 2019 , ' Retinal Pigment Epithelial Cell Line with Fast Differentiation and Improved Barrier Properties ' ,
Pharmaceutics , vol. 11 , no. 8 , 412 . <https://doi.org/10.3390/pharmaceutics11080412>

<http://hdl.handle.net/10138/305637>

<https://doi.org/10.3390/pharmaceutics11080412>

cc_by

publishedVersion

Downloaded from Helda, University of Helsinki institutional repository.

This is an electronic reprint of the original article.

This reprint may differ from the original in pagination and typographic detail.

Please cite the original version.

Article

Retinal Pigment Epithelial Cell Line with Fast Differentiation and Improved Barrier Properties

Laura Hellinen ¹, Lea Pirskanen ¹, Unni Tengvall-Unadike ¹, Arto Urtti ^{1,2,3} and Mika Reinisalo ^{1,4,*}

¹ School of Pharmacy, Faculty of Health Sciences, University of Eastern Finland, 70210 Kuopio, Finland

² Drug Research Programme, Division of Pharmaceutical Biosciences, Faculty of Pharmacy, University of Helsinki, P.O. Box 56, FI-00014 Helsinki, Finland

³ Laboratory of Biohybrid Technologies, Institute of Chemistry, St. Petersburg State University, Peterhof, 198504 St. Petersburg, Russia

⁴ Institute of Clinical Medicine, Department of Ophthalmology, Faculty of Health Sciences, University of Eastern Finland, 70210 Kuopio, Finland

* Correspondence: mika.reinisalo@uef.fi

Received: 27 June 2019; Accepted: 2 August 2019; Published: 13 August 2019



Abstract: Retinal pigment epithelium (RPE) acts as an outer blood–retinal barrier that limits the access of circulating xenobiotics to the eye. In addition, the RPE limits posterior elimination of intravitreally injected drugs to circulation. Thus, permeation in the RPE has a significant effect on ocular pharmacokinetics. The RPE is also a potentially important drug target in age-related macular degeneration. Therefore, the cell models of the RPE are important tools in ocular drug development, but poor availability and problems in reproducibility limit the use of primary RPE cell cultures. Furthermore, the best and widely used human cell line ARPE19 requires specialized culture conditions and a long time for cellular differentiation. In this paper, we describe a cell population arisen from the ARPE19 culture, with fast differentiation and improved barrier properties. This cell line, LEPI, forms clear microvilli and rapidly displays RPE-like cobblestone morphology after subculture in simple culture conditions. The LEPI cells show RPE-specific functions and expression of RPE65, ezrin, and BEST1 proteins. On filter, the LEPI cells develop tighter barrier than the ex vivo bovine RPE-choroid: permeability coefficients of beta-blockers (atenolol, nadolol, timolol, pindolol, metoprolol, betaxolol) ranged from 0.4×10^{-6} cm/sec to 2.3×10^{-6} cm/sec depending on the drug lipophilicity. This rapidly differentiating cell line will be an asset in ocular studies since it is easily maintained, it grows and differentiates quickly and does not require specialized culture conditions for differentiation. Thus, this cell line is suitable for both small scale assays and high throughput screening in drug discovery and development.

Keywords: retinal pigment epithelium; outer blood–retinal barrier; cell line; ARPE19; differentiation; tight junctions; microvilli; drug permeation; beta-blockers

1. Introduction

Retinal pigment epithelium (RPE) separates the choroidal blood flow from the neural retina, thereby forming the outer part of the blood–retinal barrier. The RPE has an important role in ocular pharmacokinetics since the inter-cellular tight junctions restrict the distribution of drugs and other xenobiotics from the choroidal bloodstream into the inner parts of the eye [1,2]. The RPE also supports visual functions; for instance, it maintains optimal ion balance in the sub-retinal space that supports the well-being of the photoreceptors of the neural retina. The RPE secretes growth factors, participates in retinoid cycling, phagocytoses shed photoreceptor outer segments (POS) and provides nutrients for

the neural retina [1]. Disturbances in RPE functions are involved in many sight-threatening diseases, such as diabetic retinopathy and age-related macular degeneration (AMD) [3] making the RPE subject to intensive medical and pharmaceutical research.

The ARPE19 cell line is widely used as a cell model of the RPE. This cell line spontaneously differentiated from a primary human RPE cell culture [4]. The original ARPE19 study showed cobblestone morphology, formation of tight junctions and microvilli, and expression of RPE-specific genes (RPE65, CRALBP) in the cell cultures [4]. Furthermore, the differentiated ARPE19 cells on filter showed polarized secretion of vascular endothelial growth factor (VEGF) and pigment epithelium-derived factor (PEDF) [5]. Permeation of test compounds across differentiated ARPE19 cells on filter was dependent on the molecular size and lipophilicity of the solutes, but the ARPE19 cultures were more permeable than isolated bovine RPE-choroid specimens [6,7]. The ARPE19 cell model also displays a similar, but not identical, transporter expression profile with human primary RPE cells (hfRPE cells) [8]. Compared to another human RPE cell line (D407), ARPE19 is considered to be a better model, since ARPE19 can form tight junctions that were not detected in D407 cultures [9]. Since the use of primary RPE cultures is limited by restricted availability of the cells, limited passaging and problems of reproducibility, ARPE19 cell line has become a widely used alternative model. However, differentiation of ARPE19 cells takes a long time (1–4 months) both on filters [5,6,10] and in the regular culture dishes [8,10,11]. Furthermore, the reported properties of the ARPE19 cell line vary between different laboratories as the original phenotype of the cell line has undergone a degradation among passaging [9]. Therefore, different routines (culture surfaces, medium composition, seeding densities, culture times) are used to restore the proper phenotype. Some studies have reported a loss of RPE specific phenotype due to the downregulation or lack of RPE-specific gene expression (e.g., RPE65) [10,12], and the gene expression of ARPE19 cells varies in different culture conditions [13].

Recently, we observed a distinct cobblestone cell population in our ARPE19 cultures that were maintained in regular culture medium on un-coated culture dishes. Due to the fast proliferation of these cuboidal RPE-like cells, they gradually overcame the ARPE19 cells in the cultures. Herein, we describe the characterization of this new ARPE19 derived cell line that was named LEPI. This cell model has significant advantages making it an attractive research tool in RPE research.

2. Materials and Methods

2.1. Cell Culture

After recognition of the morphologically different cell population among the ARPE19 cultures (at passage 27, product CRL-2302, American Type Culture Collection, ATCC, Manassas, VA, USA), the cells were sub-cultured at several seeding densities (1:10, 1:15, and 1:30) with trypsin-EDTA (0.05%, Gibco, Thermo Fisher Scientific, Waltham, MA, USA). After this passage (p-28), the cell population consisted only of the cells with cobblestone morphology on all cell plates. The culture routine was changed to lower sub-culture densities as the cells expanded into confluency in 2 to 4 days after seeding. After passage 28, the cells were identified as LEPI cells, and their passage number was switched to 1. All the studies described in this paper have been conducted with LEPI cells of passages 2 to 17. We have not done experiments with cells beyond passage 17, but we do not anticipate major differences in later passages in LEPI cells maintaining their cobblestone morphology.

The routine culture of the LEPI cells involves weekly sub-culture with 1:30 to 1:50 seeding densities and maintenance in DMEM-F12 medium (Gibco, Thermo Fisher Scientific) with 10% fetal bovine serum (FBS; Gibco, Thermo Fisher Scientific), 1% penicillin-streptomycin and 2 mM l-glutamine (both from Euroclone, Pero, Italy). The same medium composition was used with the regular ARPE19 cell culture in our laboratory.

Human primary RPE cells (hfRPE cells, HRPEpiC, ScienCell, Carlsbad, CA, USA) were expanded and cultured, as described previously [8].

Identity of all three RPE models (ARPE19, LEPI, hRPE) was examined using short-tandem repeat profiling (STR). STR analysis and profiling against the ATCC's cell STR database was conducted as Cell Line Authentication service in ATCC as described previously [14].

2.2. Transmission and Scanning Electron Microscopy

For transmission electron microscopy (TEM: JEM2100F, JEOL Ltd., Tokyo, Japan), ARPE19 (105,000 cells/cm²), LEPI (105,000 cells/cm²) and HRPEpiC (hRPE cells, 210,000 cells/cm²) cells were seeded on 24 well plates. For scanning electron microscopy (SEM; Sigma HD|VP, Carl Zeiss Microscopy GmbH, Jena, Germany), the cells were seeded on glass coverslips in 24 well plates at the same cell density as in TEM studies. After two weeks in culture, the cells were fixed, processed, and imaged at SibLabs Kuopio (Science Innovation Business Lab, Kuopio, Finland).

2.3. Immunofluorescence Staining

The LEPI cells were seeded onto ibidi μ -slides (80826, ibidi GmbH, Gräfelfing, Germany) and cultured for 18 days before the immunofluorescence staining for the RPE-specific proteins and 7 days before characterization of the fluid-filled domes. The cells were fixed with 100% methanol (at -20°C) and stained with primary antibodies for immunofluorescence (Table 1) together with specific Alexa Fluor secondary antibodies (Thermo Fisher Scientific). Cell nuclei were stained with 1:10,000 dilution of DAPI (D9542 Sigma Aldrich, Saint Louis, MO, USA) and visualized with Zeiss LSM 800 Airyscan confocal microscope (Carl Zeiss LSM 800, Carl Zeiss Microscopy GmbH, Jena, Germany).

Table 1. The antibody information.

Primary Antibody	Cat n:o and Vendor	Dilution	Secondary Antibody	Cat n:o and Vendor	Dilution
ezrin	sc-58758, Santa Cruz Biotechnology	1:100	goat anti-mouse AF594	A-11032 Thermo Fischer Scientific	1:1000
occludin	71-1500, Thermo Fischer Scientific	1:100	goat anti-rabbit AF488	A-11034 Thermo Fischer Scientific	1:1000
RPE65	NB100-355, Novus Biologicals	1:100	goat anti-mouse AF594	A-11032 Thermo Fischer Scientific	1:1000
MRP1	ab3368, Abcam	1:100	goat anti-Rat AF568	A-11029 Thermo Fischer Scientific	1:1000

2.4. Phagocytosis Assay

Isolation of photoreceptor outer segments (POS) from porcine eyes and labeling with fluorescein isothiocyanate (FITC) was carried out as described earlier [8] (Supplement: Characterization of human fetal retinal pigment epithelial (hRPE) cells).

For phagocytosis assay, the cells were seeded on ibidi μ -slides (80826) at cell density 45,000 cells/cm². After culturing for one week, the cells were incubated with 10 μg of labeled FITC-POS/cm² for 20 h. After incubation, the cells were washed four times with PBS to remove all FITC-POS that had not been phagocytosed. Eventually, the cells were fixed and counterstained with MRP1 antibody as described above (Immunofluorescence staining).

2.5. Doubling Time

The proliferation of ARPE19 and LEPI cells was characterized by cell doubling-time assays. For the assay, the cells were seeded onto 6-well plates at low density (0.15 million cells/well). After 48 h and at the sub-confluent stage, the cells were detached by trypsinization and counted with Bürker hemocytometer. The doubling times of the cell lines were calculated using Equation (1).

$$DT = T \ln 2 / \ln(X_e/X_b), \quad (1)$$

where T is the incubation time, \ln stands for the natural logarithm, X_b is the cell number at the start, and X_e is the cell number at the end of the culturing.

2.6. Permeability Studies

For the permeability experiments, the cells were seeded at 160,000 cells/cm² onto 1.12 cm² polyester filters with 0.4 µm pore size (3460-Clear Transwells, Corning Inc., Corning, NY, USA). The cells were cultured for 1 to 4 weeks in DMEM-F12 containing 1% FBS, 1% penicillin-streptomycin, and 2 mM l-glutamine, and the growth medium was replaced 3 times a week. The same procedure was used for both regular ARPE19 and LEPI cells.

The permeation was studied in apical-to-basolateral direction. Mannitol (³H-labeled mannitol, Perkin Elmer, Waltham, MA, USA) was used as a paracellular marker. Permeability of atenolol, metoprolol, nadolol, pindolol, timolol (all from Sigma Aldrich) and betaxolol (Alcon, Fort Worth, TX, USA) was investigated. The permeability assay with mannitol was conducted with LEPI and ARPE19 cultures (original ATCC's product CRL-2302). The beta-blocking drugs (atenolol, metoprolol, nadolol, pindolol, timolol, betaxolol) were administered as cassette solution, with 10 µM of each drug in HBSS-Hepes (10 mM) buffer (pH 7.40). The experiments took place at 37 °C, and the cells were kept on low-speed shaking (170 rpm Heidolph incubator 1000 and Titramax 1000, Heidolph Electro GmbH & Co., Keiheim, Germany). The permeation was monitored by sampling the receiver phase at 15, 30, 45, 60, 75, 90, 120, 150, 180, 210, 240, 270, 300, 330, and 360 min.

The apparent permeability coefficients P_{app} (in cm/sec) were calculated with Equation (2) below.

$$P_{app} = J/(C_0 \times A), \quad (2)$$

where J is the drug flux (ng/sec or cpm/sec) across the cell monolayer, C_0 (ng/cm³ or cpm/cm³) is the starting concentration, and A is the monolayer surface area (1.12 cm²). The sink conditions were maintained during the linear phase of permeation. At that stage drug concentration in the receiver compartment was maintained below 10% of the concentration in the donor compartment.

2.7. Drug Concentration Determination

The radioactivity counts of ³H-mannitol were determined with a liquid scintillation counter (Microbeta Plus 1450, Perkin Elmer, Waltham, MA, USA) after equilibrating the samples overnight in Ultima Gold[®] solution (Perkin Elmer).

The beta-blocker concentrations were analyzed with LC-MS/MS with previously described methods [15,16] using a liquid chromatograph (Agilent 1290, Agilent Technologies, Inc., Santa Clara, CA, USA) and a triple-quadrupole mass spectrometer (Agilent 6495; Agilent Technologies, Inc., Santa Clara, CA, USA) with electrospray ionization. The validation of the compound analysis has been described in detail in our previous publications [15,16], and similar measures were undertaken to validate the LC-MS/MS runs.

3. Results

3.1. Morphology of Rapidly Growing LEPI Cells Is Similar to Primary RPE Cultures

We observed round colonies with distinct cobblestone morphology in our regular ARPE19 cell plates in passage 27 (Figure 1a,b). The morphology is different from regular ARPE19 cells, which are clearly longer (Figure 1a–c), and the difference can be seen immediately after sub-culture (Figure 1c,d). The LEPI cells retained their cuboidal morphology, even at low seeding densities (Figure 1d,e). The authentication assay conducted by ATCC showed that the LEPI and ARPE19 cells are of the same origin (Supplementary Materials) confirming that the LEPI cells are not a contamination from another cell line.

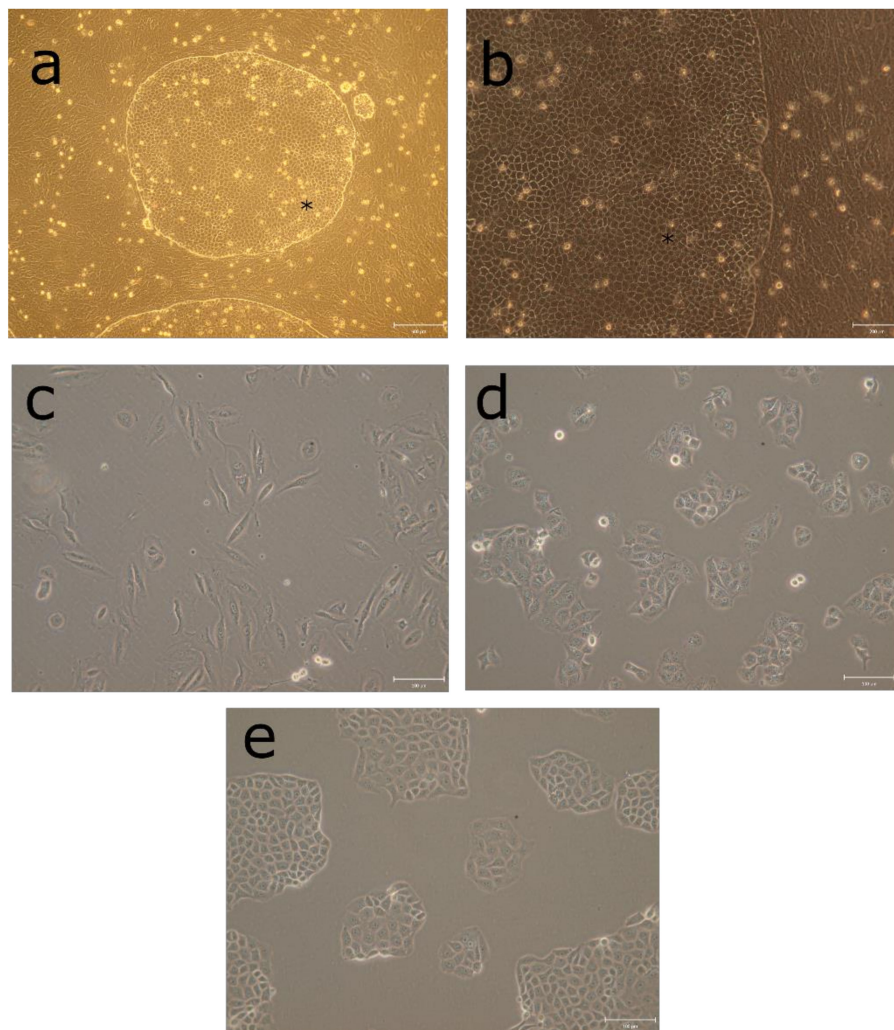


Figure 1. ARPE19 derived LEPI cells with cobblestone morphology arose from regular ARPE19 cultures. The round cell colonies containing the LEPI cell population (marked with *) inside the ARPE19 cultures showed distinct morphology compared to regular ARPE19 cells (a,b). At low culture densities, the regular ARPE19 cells (c) display more spindle shape morphology compared to LEPI cells (d) that instantly displayed cuboidal epithelial-like phenotype at 24 h after sub-culturing. The cells start to display RPE-like morphology 3 days after sub-culturing at 1:30 density (e). Scale bars (a) 500 μ M, (b) 200 μ M, (c–e) 100 μ M.

Scanning electron microscopy revealed that LEPI cells (Figure 2e) and hRPE cells (Figure 2c) form clear microvilli, whereas microvilli were not detected in ARPE19 cells (Figure 2a). Transmission electron micrographs demonstrate the presence of tight junctions in each cell model (Figure 2b,d,f). LEPI (Figure 2f) and ARPE19 (Figure 2b) cells did not have pigmentation, whereas small vesicles, which can be pre-melanosomes, were detected in hRPE cells (Figure 2d).

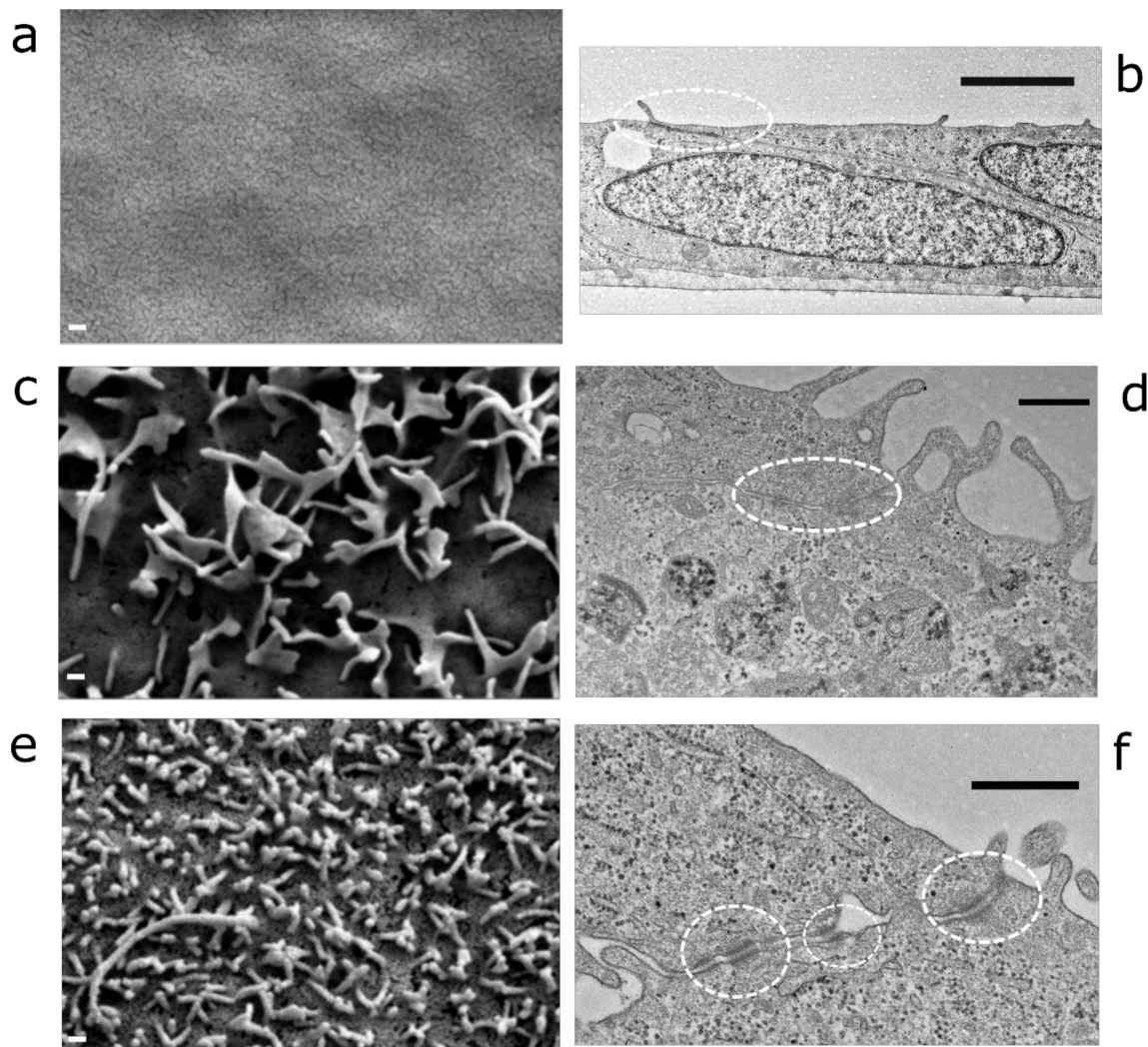


Figure 2. LEPI cells form similar tight junctions and microvilli with primary RPE cells. SEM imaging was used to evaluate the microvilli formation (a,c,e). ARPE19 cells (a) do not form clear microvilli, whereas hRPE cells (c) and LEPI cells (e) display microvilli. Scale bars of SEM images (a,c,e) are 200 nm. The TEM images show tight junctions (circled) in ARPE19 (b), hRPE (d) and LEPI cells (f). ARPE19 TEM image scale bar is 2 μ m (b), and the LEPI (f) and hRPE (d) image scale bars are 500 nm.

3.2. LEPI Cells Display RPE-Specific Protein Expression and Function

We detected protein expression involved with tight junctions (occludin, Figure 3) and microvilli (ezrin, Figure 3a) in LEPI cells. In addition, LEPI cells displayed RPE-specific protein expression (RPE65, BEST1 Figure 3b,c) indicating proper cellular maturation. The cells also formed fluid-filled domes that confirm proper apical-to-basolateral polarity and the presence of tight junctions (Figure 4). Furthermore, the cells phagocytosed FITC-labeled photoreceptor outer segments that were isolated from the porcine neural retina (Figure 3d).

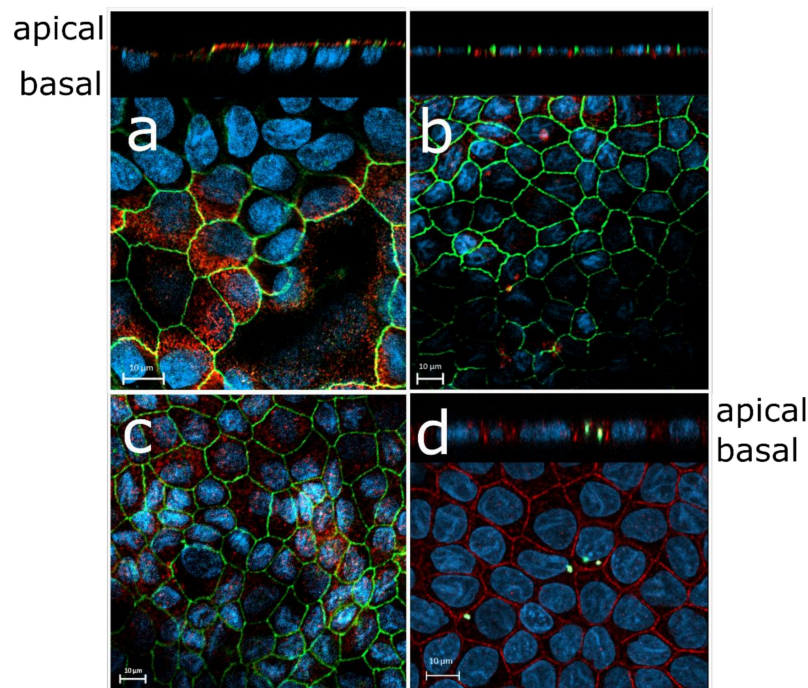


Figure 3. LEPI cells with mature RPE phenotype. Occludin was used in all (a–c) images to reveal the cell shape and the presence of tight junctions (green). DAPI stain was used to visualize the cell nuclei (blue). (a) Ezrin (red) was detected on the apical surface indicating proper microvilli formation. (b) LEPI cells showed RPE-specific BEST1 expression on the basal membrane (red) and (c) RPE65 expression in the cytoplasm (red). The cells were cultured 18 days before imaging. (d) Confocal microscope image of LEPI cells cultured on Ibidi slides for one week. The cells were exposed to FITC labeled photoreceptor outer segments (FITC-POS, green), and after 20 h incubation, the cells were washed and counterstained with anti-MRP1 antibody (red) localized in lateral plasma membranes. The vertical section view (upper panel) shows internalized FITC-POS in LEPI cells. Scale bars 10 μm .

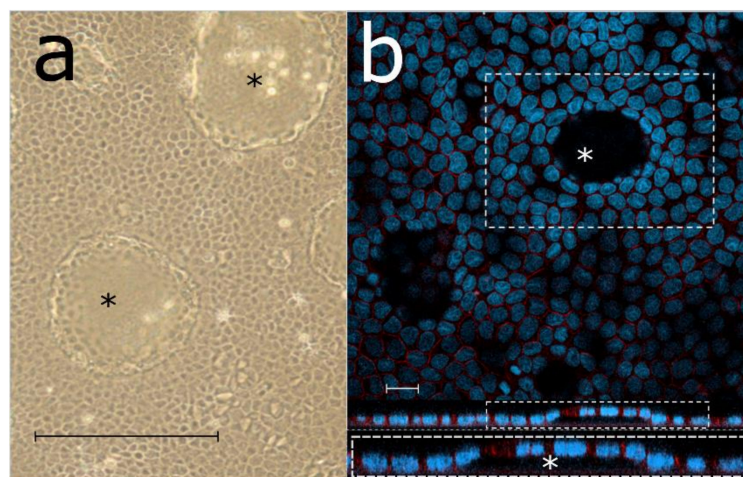


Figure 4. As evidence for cellular polarity and presence of tight-junctions, increased number of fluid-filled domes (*) were formed in LEPI cell cultures after 7 days of culturing. (a) Bright-field image of LEPI cells on a culture dish. Scale bar 500 μm (b) Confocal microscope image of immunofluorescence stained LEPI cells on ibidi slide, scale bar 20 μm . Lateral plasma membranes counterstained with multi-drug resistance associated protein 1 (MRP1, red) and DAPI stained cell nuclei (blue). Inset of boxed area displaying X-Z section view (apical/basal sides) of the fluid-filled dome (*) in the cell monolayer. The domes are seen as holes in the images that display the top view of the culture. The cells at that z-level are located above the section that is in focus (*).

3.3. LEPI Cells Form an Appropriate Outer Blood–Retinal Barrier Model

We compared the doubling time among regular ARPE19 cells and the LEPI cells with RPE-like morphology. Based on cell proliferation assay, the LEPI cells divided 2.3 times faster than regular ARPE19 cells (Figure 5a), but the growth of LEPI cells is controlled by contact inhibition, and these cells grow as a monolayer.

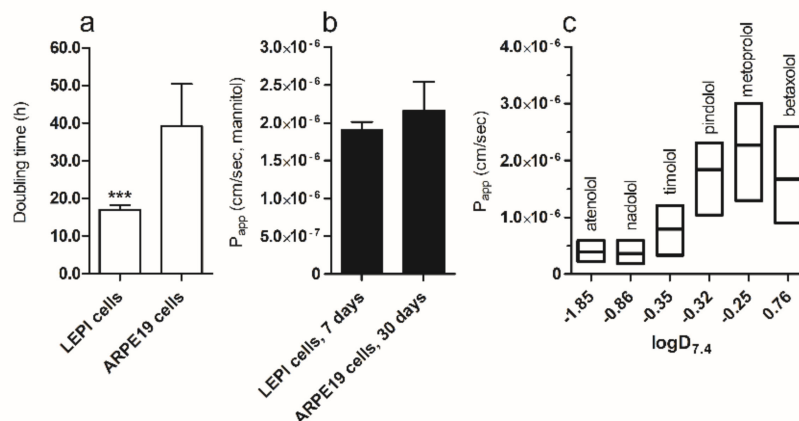


Figure 5. Doubling time and barrier formation of LEPI cells is faster than regular ARPE19 cells. (a) Comparison between LEPI and ARPE19 cells shows that cell division rate of LEPI cells is 2.3 times faster than that of regular ARPE19 cells ($n = 12$, *** $p < 0.0001$, determined with unpaired t -test with Welch's correction). The results are presented as the mean doubling-time \pm standard deviation (SD) from four independent cultures, each performed in triplicate. (b) LEPI cells ($n = 7$) form a barrier against paracellular permeation similar to ARPE19 cells ($n = 5$). The apparent permeability coefficient (P_{app}) of mannitol was similar in LEPI cells after culture of 7 days and in ARPE19 cells that were cultured for 30 days. The bars display average values and error bar standard deviation (SD). (c) The permeation of beta-blockers across the tight LEPI monolayers (cultured for 30 days) is related to compound lipophilicity. The apparent permeability coefficients (P_{app}) are displayed as a range, and the lines represent the average values ($n = 3$).

Since LEPI cells seemed to gain differentiated phenotype quickly in culture, we compared their barrier properties after one week in culture to ARPE19 cells that had been cultured on filters for 30 days (Figure 5b). LEPI cells form a barrier against paracellular diffusion in one week, as the apparent permeation coefficients (P_{app}) of mannitol were similar in these two cases (Figure 5b). However, we recorded even lower mannitol permeation values after 4-week LEPI-cultures ($<0.9 \times 10^{-6}$ cm/s, data not shown) and thus, decided to perform the further barrier evaluation with cells cultured for 4 weeks.

The beta-blockers showed different permeation rates across the LEPI cell layer (Figure 5c). The drug permeation in the LEPI cultures showed the similar rank-order as their lipophilicities ($\log D_{7.4}$ values, Figure 5c, and Table 2) and the P_{app} values in isolated bovine RPE-choroid (Table 2). The P_{app} values of beta-blockers are 1.9- to 10.8-fold lower in LEPI cells than in the isolated RPE-choroid (Table 2).

Table 2. Permeability of drugs across LEPI cells and bovine RPE-choroid.

Compound	logD _{7.4} (Predicted, ACDLabs) ¹	P _{app} across LEPI Cells ± SD (×10 ^{−6} cm/s, Apical-to-Basolateral)	P _{app} across Bovine RPE-Choroid ² ± SD (×10 ^{−6} cm/s, Apical-to-Basolateral)	Fold Differences in P _{app} (RPE-Choroid/LEPI)
atenolol	−1.85	0.39 ± 0.15 *	2.00 ± 0.47	5.1
nadolol	−0.86	0.37 ± 0.17 *	2.03 ± 0.46	5.5
timolol	−0.35	0.78 ± 0.34	8.41 ± 2.7	10.8
pindolol	−0.32	1.8 ± 0.57	3.48 ± 1.7	1.9
metoprolol	−0.25	2.3 ± 0.68	10.6 ± 3.2	4.6
betaxolol	0.76	1.7 ± 0.68	10.3 ± 3.7	6.1

¹ Values collected from the ChemSpider database (Royal Society of Chemistry); ² Values reported by [7]. * Significantly different from metoprolol ($p < 0.05$, determined with one-way ANOVA and the Holm–Sidak method. The LEPI P_{app} data passed the normality and equal variance criteria determined with Shapiro–Wilk and Brown–Forsythe methods, respectively).

4. Discussion

In this study, we present an RPE cell line, LEPI, that differentiates within 1 to 4 weeks after sub-culture into a phenotype similar to primary RPE. Unlike the ARPE-19 cells, the LEPI cells rapidly form cobblestone morphology, clear microvilli, and tight barrier in simple culture conditions. As expected the LEPI and ARPE19 cells show an exact authentication match with the original ARPE19 cell line (Supplementary Materials), and as expected, the hfRPE cells did not have any matches in the ATCC’s STR database. Cobblestone morphology can be achieved in ARPE19 cultures, but this requires months in culture and specialized culture conditions [5,10].

4.1. Morphology and RPE-Specific Protein Expression of LEPI Cells Reveal the Differentiated Phenotype

LEPI cells display a cobblestone phenotype quickly after sub-culture (Figure 1e), and they even form domes (Figure 4) that have been associated with differentiated phenotype with proper polarity and tight junctions in hfRPE cultures [8,17]. We compared the microvillus formation by SEM and showed that LEPI cells form distinct microvilli (Figure 2e), whereas it was lacking from regular ARPE19 cells according to SEM images (Figure 2a). Ezrin protein expression on the apical cell surface further confirmed that the LEPI cells form appropriate microvilli (Figure 3a). Tight junctions were detected in all studied cell models (Figure 2b,d,e and Figure 3a–c; occludin expression in lateral surfaces of LEPI cells), and the TEM image revealed that ARPE19 cells do not grow as a true monolayer since the cellular lateral surfaces are diagonal (Figure 2b). The pigmentation is lacking from the LEPI cells (Figure 2f), but the existing RPE cell lines (ARPE19, D407) do not contain pigment either. The hfRPE cells displayed only modest pigmentation (Figure 2d) compared to highly pigmented native RPE [18]. Overall, the morphology of the LEPI cells is similar to ARPE19 cells that differentiated to RPE-like phenotype in earlier studies after 2.5 to 4 months [5,13]. We confirmed the mature RPE phenotype of LEPI cells with RPE-specific marker protein expression (BEST1 on the basal surface, RPE65 in the cytoplasm; Figure 3b,c). Importantly, the cells phagocytosed the photoreceptor outer segments (Figure 3d) verifying differentiated RPE-specific phenotype. Phagocytosis of the daily shed photoreceptor outer segments is one of the key RPE functions maintaining the optimal conditions in the sub-retinal space [1].

Epithelial-mesenchymal transition (EMT) has been suggested to cause the dedifferentiated ARPE19 phenotype [10]. The same phenomenon may take place also in hfRPE cultures if the cell–cell contacts are lacking due to too low sub-culture density [17,19]. Interestingly, LEPI cells seem to be resistant towards EMT, as their appearance is epithelial-associated (“cobblestone-like”) already 3 days after sub-culturing even at low seeding densities (<10% of the culture plate, Figure 1e). The clear morphological difference among regular ARPE19 and LEPI cells is evident immediately after sub-culture: ARPE19 cells are fibroblast-like, whereas LEPI cells have cuboidal, epithelial shape 24 h after sub-culture (Figure 1c,d). In

addition, the growth of LEPI cells is 2.3 times faster than that of ARPE19 cells (Figure 5a). Due to its fast differentiation and ability to divide faster than the regular ARPE19 cells, LEPI cells are more convenient to maintain and easily expanded for assays requiring large cell quantities than regular ARPE19. Rapid differentiation without specialized culture medium makes the cell model cost-effective. These aspects make LEPI cells suitable for high throughput assays in retinal biology and drug discovery.

4.2. LEPI Cells Are Suitable as an Outer Blood–Retinal Barrier Model

When we compared LEPI cell population to regular ARPE19 cells, we discovered that the LEPI cells form a tight barrier in 7 days, while it takes 30 days for the ARPE19 cells to generate a comparable barrier (Figure 5b). Paracellular permeation in the apical-to-basolateral direction in LEPI cells was similar to paracellular permeability in bovine RPE-choroid explants in the basolateral-to-apical direction (mannitol P_{app} approximately $(1-2) \times 10^{-6}$ cm/s) [20]. Thus, the permeation set-up with LEPI cells is equivalent to the RPE-choroid tissue in a Ussing chamber as an outer blood–retinal barrier model.

Previously Mannermaa et al. [6] investigated ARPE19 cells as an outer blood–retinal barrier model. They reported drug permeation values that were dependent on the molecular size and lipophilicity of the permeants, but the P_{app} values of betaxolol, 6-carboxyfluorescein, and 40 kDa FITC-dextran were 3.2, 7.6, and 17.1 times higher than in the bovine RPE-choroid tissues, respectively [7]. As ARPE19 cells kept in culture for 4 weeks still display a leaky barrier, and mannitol permeation after only one-week culture was similar to 4-week ARPE19 culture (Figure 5b), we decided to further characterize the permeation properties of the LEPI cells cultured for 4 weeks.

We aimed to define the capability of LEPI cells to re-produce the relationship between the compound lipophilicity and permeability that was observed earlier in the bovine RPE-choroid [7]. For that purpose, we used the same compounds (atenolol, nadolol, timolol, pindolol, metoprolol, and betaxolol) as described in an earlier report [7]. These beta-blocking agents have a similar molecular weight of 250 to 320 Da and pK_a values around 9, but their $\log D_{7.4}$ values have a wide range from -1.85 to $+0.76$ (Table 2). As in bovine RPE-choroid [7], the lipophilic beta-blockers (metoprolol and betaxolol) permeated faster in the LEPI cultures than the hydrophilic compounds (atenolol, nadolol). The difference between the high (e.g., metoprolol) and low permeability compounds (e.g., nadolol) was 6.2-fold in LEPI cells. The lipophilic drugs can permeate across the cellular lipid bilayer more easily than hydrophilic ones as they can pass through the cell membranes, in addition to the paracellular route.

We also compared the permeation of the beta-blockers across the LEPI monolayer with the published permeability values in the bovine RPE-choroid [7]. The LEPI cells did not only reproduce the rank order of P_{app} values observed in bovine RPE-choroid experiments [7] (Figure 5c) but also displayed tighter barrier as the P_{app} values were 2 to 19 times lower in LEPI cells than in the bovine RPE-choroid (Table 2). Similar to our observations, Caco-2 cells cultured and studied on transwells also display lower P_{app} values compared to human intestinal tissue studied with a Ussing chamber system [21]. Even with this difference in observed experimental values, and the lack of linear correlation in P_{app} values with Caco-2 and human intestine, the Caco-2 cell line is a valuable tool that is widely used to predict the oral drug absorption in humans. Overall, LEPI cells constitute a promising model for the outer blood–retinal barrier, because they form a tighter barrier than differentiated ARPE19 cells [6] and isolated bovine RPE-choroid [7,20]. Furthermore, the LEPI cells correctly demonstrate the impact of permeant lipophilicity on membrane permeability. Further work is needed to establish the cause of rapid growth and differentiation rate of LEPI cells. Comparison of epigenetic regulation of ARPE19 and LEPI cells might reveal the difference, and lead to improved understanding of the RPE development and biology.

5. Conclusions

In conclusion, we present new RPE cell model with improved barrier properties and mature RPE phenotype. Our cell model is easy to handle without the need for specialized culture conditions and

long differentiation times. In addition, LEPI cells divide and expand rapidly, making this new cell model superior to regular ARPE19 in drug discovery and development.

Supplementary Materials: The following are available online at <http://www.mdpi.com/1999-4923/11/8/412/s1>. Supplementary Materials: The cell line authentication by ATCC (PDF-file).

Author Contributions: Conceptualization, L.H., A.U. and M.R.; methodology, L.H., L.P., U.T.-U., M.R.; validation, L.H., U.T.-U., M.R. formal analysis, L.H.; investigation, L.H., L.P., U.T.-U. and M.R.; resources, A.U.; data curation, L.H. and M.R.; writing—original draft preparation, L.H.; writing—review and editing, L.H., A.U., M.R.; visualization, L.H. and M.R.; supervision, A.U. and M.R.; project administration, L.H. and M.R.; funding acquisition, A.U.

Funding: This research was funded by Academy of Finland, grant number 311122, Finnish Cultural Foundation (personal grant for L.H.) and Government of Russian Federation Mega-Grant, grant number 14.W03.031.0025 “Biohybrid technologies for modern biomedicine” (A.U.).

Acknowledgments: We thank Science Innovation Business Labs Kuopio and Arto Koistinen for performing the electronic microscopic examinations. We would like to thank Linne Koskela (M. Sc.) for the contribution in the ARPE19 permeation assays.

Conflicts of Interest: The authors declare no conflict of interest.

References

1. Strauss, O. The Retinal Pigment Epithelium in Visual Function. *Physiol. Rev.* **2005**, *85*, 845–881. [CrossRef] [PubMed]
2. Del Amo, E.M.; Rimpela, A.K.; Heikkinen, E.; Kari, O.K.; Ramsay, E.; Lajunen, T.; Schmitt, M.; Pelkonen, L.; Bhattacharya, M.; Richardson, D.; et al. Pharmacokinetic Aspects of Retinal Drug Delivery. *Prog. Retin. Eye Res.* **2017**, *57*, 134–185. [CrossRef] [PubMed]
3. Pavan, B.; Dalpiaz, A. Retinal Pigment Epithelial Cells as a Therapeutic Tool and Target Against Retinopathies. *Drug Discov. Today* **2018**, *23*, 1672–1679. [CrossRef] [PubMed]
4. Dunn, K.C.; Aotaki-Keen, A.E.; Putkey, F.R.; Hjelmeland, L.M. ARPE-19, a Human Retinal Pigment Epithelial Cell Line with Differentiated Properties. *Exp. Eye Res.* **1996**, *62*, 155–169. [CrossRef] [PubMed]
5. Shadforth, A.M.A.; Suzuki, S.; Theodoropoulos, C.; Richardson, N.A.; Chirila, T.V.; Harkin, D.G. A Bruch’s Membrane Substitute Fabricated from Silk Fibroin Supports the Function of Retinal Pigment Epithelial Cells in Vitro. *J. Tissue Eng. Regen. Med.* **2017**, *11*, 1915–1924. [CrossRef] [PubMed]
6. Mannermaa, E.; Reinisalo, M.; Ranta, V.P.; Vellonen, K.S.; Kokki, H.; Saarikko, A.; Kaarniranta, K.; Urtti, A. Filter-Cultured ARPE-19 Cells as Outer Blood-Retinal Barrier Model. *Eur. J. Pharm. Sci.* **2010**, *40*, 289–296. [CrossRef]
7. Pitkanen, L.; Ranta, V.P.; Moilanen, H.; Urtti, A. Permeability of Retinal Pigment Epithelium: Effects of Permeant Molecular Weight and Lipophilicity. *Invest. Ophthalmol. Vis. Sci.* **2005**, *46*, 641–646. [CrossRef]
8. Pelkonen, L.; Sato, K.; Reinisalo, M.; Kidron, H.; Tachikawa, M.; Watanabe, M.; Uchida, Y.; Urtti, A.; Terasaki, T. LC-MS/MS Based Quantitation of ABC and SLC Transporter Proteins in Plasma Membranes of Cultured Primary Human Retinal Pigment Epithelium Cells and Immortalized ARPE19 Cell Line. *Mol. Pharm.* **2017**, *14*, 605–613. [CrossRef]
9. Rizzolo, L.J. Barrier Properties of Cultured Retinal Pigment Epithelium. *Exp. Eye Res.* **2014**, *126*, 16–26. [CrossRef]
10. Samuel, W.; Jaworski, C.; Postnikova, O.A.; Kutty, R.K.; Duncan, T.; Tan, L.X.; Poliakov, E.; Lakkaraju, A.; Redmond, T.M. Appropriately Differentiated ARPE-19 Cells Regain Phenotype and Gene Expression Profiles Similar to those of Native RPE Cells. *Mol. Vis.* **2017**, *23*, 60–89.
11. Philp, N.J.; Wang, D.; Yoon, H.; Hjelmeland, L.M. Polarized Expression of Monocarboxylate Transporters in Human Retinal Pigment Epithelium and ARPE-19 Cells. *Invest. Ophthalmol. Vis. Sci.* **2003**, *44*, 1716–1721. [CrossRef] [PubMed]
12. Strunnikova, N.V.; Maminishkis, A.; Barb, J.J.; Wang, F.; Zhi, C.; Sergeev, Y.; Chen, W.; Edwards, A.O.; Stambolian, D.; Abecasis, G.; et al. Transcriptome Analysis and Molecular Signature of Human Retinal Pigment Epithelium. *Hum. Mol. Genet.* **2010**, *19*, 2468–2486. [CrossRef] [PubMed]

13. Tian, J.; Ishibashi, K.; Honda, S.; Boylan, S.A.; Hjelmeland, L.M.; Handa, J.T. The Expression of Native and Cultured Human Retinal Pigment Epithelial Cells Grown in Different Culture Conditions. *Br. J. Ophthalmol.* **2005**, *89*, 1510–1517. [[CrossRef](#)] [[PubMed](#)]
14. Capes-Davis, A.; Reid, Y.A.; Kline, M.C.; Storts, D.R.; Strauss, E.; Dirks, W.G.; Drexler, H.G.; MacLeod, R.A.; Sykes, G.; Kohara, A.; et al. Match Criteria for Human Cell Line Authentication: Where do we Draw the Line? *Int. J. Cancer* **2013**, *132*, 2510–2519. [[CrossRef](#)] [[PubMed](#)]
15. Ramsay, E.; Ruponen, M.; Picardat, T.; Tengvall, U.; Tuomainen, M.; Auriola, S.; Toropainen, E.; Urtti, A.; Del Amo, E.M. Impact of Chemical Structure on Conjunctival Drug Permeability: Adopting Porcine Conjunctiva and Cassette Dosing for Construction of in Silico Model. *J. Pharm. Sci.* **2017**, *106*, 2463–2471. [[CrossRef](#)] [[PubMed](#)]
16. Pelkonen, L.; Tengvall-Unadike, U.; Ruponen, M.; Kidron, H.; Del Amo, E.M.; Reinisalo, M.; Urtti, A. Melanin Binding Study of Clinical Drugs with Cassette Dosing and Rapid Equilibrium Dialysis Inserts. *Eur. J. Pharm. Sci.* **2017**, *109*, 162–168. [[CrossRef](#)] [[PubMed](#)]
17. Adijanto, J.; Philp, N.J. Cultured Primary Human Fetal Retinal Pigment Epithelium (hfRPE) as a Model for Evaluating RPE Metabolism. *Exp. Eye Res.* **2014**, *126*, 77–84. [[CrossRef](#)]
18. Oganessian, A.; Bueno, E.; Yan, Q.; Spee, C.; Black, J.; Rao, N.A.; Lopez, P.F. Scanning and Transmission Electron Microscopic Findings during RPE Wound Healing in Vivo. *Int. Ophthalmol.* **1997**, *21*, 165–175. [[CrossRef](#)]
19. Tamiya, S.; Liu, L.; Kaplan, H.J. Epithelial-Mesenchymal Transition and Proliferation of Retinal Pigment Epithelial Cells Initiated upon Loss of Cell-Cell Contact. *Invest. Ophthalmol. Vis. Sci.* **2010**, *51*, 2755–2763. [[CrossRef](#)]
20. Zhou, J.; He, S.; Zhang, N.; Spee, C.; Zhou, P.; Ryan, S.J.; Kannan, R.; Hinton, D.R. Neutrophils Compromise Retinal Pigment Epithelial Barrier Integrity. *J. Biomed. Biotechnol.* **2010**, *2010*, 289360. [[CrossRef](#)]
21. Westerhout, J.; Van de Steeg, E.; Grossouw, D.; Zeijdner, E.E.; Krul, C.A.; Verwei, M.; Wortelboer, H.M. A New Approach to Predict Human Intestinal Absorption using Porcine Intestinal Tissue and Biorelevant Matrices. *Eur. J. Pharm. Sci.* **2014**, *63*, 167–177. [[CrossRef](#)] [[PubMed](#)]



© 2019 by the authors. Licensee MDPI, Basel, Switzerland. This article is an open access article distributed under the terms and conditions of the Creative Commons Attribution (CC BY) license (<http://creativecommons.org/licenses/by/4.0/>).